



Published in final edited form as:

*Kidney Int.* 2016 August ; 90(2): 363–372. doi:10.1016/j.kint.2016.04.020.

## Mice with mutant *Inf2* show impaired podocyte and slit diaphragm integrity in response to protamine induced kidney injury

Balajikarthick Subramanian<sup>1,2,\*</sup>, Hua Sun<sup>1,2,3,\*</sup>, Paul Yan<sup>1</sup>, Victoria T. Charoonratana<sup>1</sup>, Henry N. Higgs<sup>4</sup>, Fang Wang<sup>1,5</sup>, Ka-Man V. Lai<sup>6</sup>, David M. Valenzuela<sup>6</sup>, Elizabeth J. Brown<sup>1,2,7,8</sup>, Johannes S. Schlöndorff<sup>1,2</sup>, and Martin R. Pollak<sup>1,2,9</sup>

<sup>1</sup>Division of Nephrology, Department of Medicine, Beth Israel Deaconess Medical Center, Boston, MA

<sup>2</sup>Harvard Medical School, Boston, MA

<sup>3</sup>Iowa University Children's Hospital, Iowa City, IA

<sup>4</sup>Department of Biochemistry, Geisel School of Medicine, Dartmouth College, Hanover, NH

<sup>5</sup>Department of Pediatrics, Peking University First Hospital, China

<sup>6</sup>Regeneron Pharmaceuticals, Inc., 777 Old Saw Mill River Road, Tarrytown, NY

<sup>7</sup>Division of Nephrology, Department of Pediatrics, Children's Hospital, Boston, MA

<sup>8</sup>Department of Pediatrics, University of Texas Southwestern Medical Center, Dallas, TX

<sup>9</sup>Broad Institute of Harvard and MIT, Cambridge, MA

### Abstract

Mutations in the *INF2* (inverted formin 2) gene, encoding a diaphanous formin family protein that regulates actin cytoskeleton dynamics, cause human focal segmental glomerulosclerosis (FSGS). *INF2* interacts directly with certain other mammalian diaphanous formin proteins (mDia) that function as RhoA effector molecules. FSGS-causing *INF2* mutations impair these interactions and disrupt the ability of *INF2* to regulate Rho/Dia-mediated actin dynamics *in vitro*. However, the precise mechanisms by which *INF2* regulates and *INF2* mutations impair glomerular structure and function remain unknown. Here, we characterize an *Inf2* R218Q point-mutant (knockin) mouse to help answer these questions. Knockin mice have no significant renal pathology or proteinuria at baseline despite diminished *INF2* protein levels. *INF2* mutant podocytes do show impaired reversal of protamine sulfate induced foot process effacement by heparin sulfate perfusion. This is associated with persistent podocyte cytoplasmic aggregation, nephrin phosphorylation, and nephrin and podocin mislocalization, as well as impaired recovery of mDia membrane

Correspondence: Martin Pollak, 99 Brookline Avenue, Boston MA 02215, mpollak@bidmc.harvard.edu, (617) 667-0461.  
\*equal contributors

**Publisher's Disclaimer:** This is a PDF file of an unedited manuscript that has been accepted for publication. As a service to our customers we are providing this early version of the manuscript. The manuscript will undergo copyediting, typesetting, and review of the resulting proof before it is published in its final citable form. Please note that during the production process errors may be discovered which could affect the content, and all legal disclaimers that apply to the journal pertain.

localization. These changes were partially mimicked in podocyte outgrowth cultures, in which podocytes from knockin mice show altered cellular protrusions compared to those from wild-type mice. Thus, in mice, normal INF2 function is not required for normal glomerular development but normal INF2 is required for regulation of the actinbased behaviors necessary for response to and/or recovery from injury.

## Keywords

cytoskeleton; glomerulus; focal segmental glomerulosclerosis

---

## Introduction

Inverted formin 2 (INF2) is a member of the formin family of actin regulatory proteins. Mutations in INF2 cause an autosomal dominant human kidney disease characterized by focal segmental glomerulosclerosis (FSGS) with or without Charcot-Marie-Tooth disease<sup>1-3</sup>. INF2 is a multidomain protein whose function depends on the regulatory effect of the N-terminal Diaphanous Inhibitory Domain (DID) on the C-terminal Diaphanous Autoregulatory Domain (DAD). In addition to INF2's actin polymerizing and depolymerizing activities, INF2 also antagonizes Rho activated actin polymerizing activity of diaphanous related formin proteins (Dias) via the interaction of the INF2 DID with mDia DAD<sup>4, 5</sup>. R218Q, a disease-causing mutation located in the DID, interferes with the INF2-DID / mDia-DAD interaction and prevents the dampening effect of INF2 on Rho/Dia signaling, leading to perturbed actin polymerization and disruption of actin based cellular remodeling processes (e.g. lamellipodia formation and plasma membrane trafficking) in cultured podocytes<sup>5, 6</sup>.

Podocyte injury is a characteristic feature of proteinuric kidney diseases. *In vivo*, podocytes branch into projections called foot processes and form specialized cell-cell junctions, slit diaphragms, that make up the distal component of the glomerular filtration barrier<sup>7, 8</sup>. The unique morphology and function of podocytes are dependent on regulation of the actin cytoskeleton, which is under the spatial and temporal control of the Rho family of small GTPases<sup>9-14</sup>. Ultrastructurally, podocytes from FSGS patients carrying the INF2 R218Q mutation show prominent actin aggregation within foot processes accompanied by loss of the normal linear distribution of slit diaphragm proteins, similar to the features of podocytes described in proteinuric transgenic mice expressing constitutively active RhoA<sup>1, 6, 9, 15</sup>. These observations are consistent with a model whereby INF2 helps fine tune the actin dynamics responsible for the normal podocyte phenotype via control of Rho/Dia signaling mediated through the INF2-DID / mDia-DAD interaction, while FSGS-causing mutations in INF2 DID prevent the normal remodeling of actin-based structures in the face of Rho/Dia activation<sup>6</sup>. To address this hypothesis and to further investigate the mechanism by which FSGS-causing INF2 mutations cause podocyte injury and FSGS *in vivo*, we generated an Inf2 R218Q point mutant knockin mouse model.

## Results

### Development of R218Q point mutant mouse

We used homologous recombination to develop mice in which the endogenous *Inf2* gene is mutated to include an R218Q amino acid substitution (Figure 1). We refer to this R218Q model as a "knockin" or "KI" mouse. The incorporation of the engineered R218Q *Inf2* mutation and normal level of transcript expression was confirmed by direct sequencing of an *Inf2* cDNA fragment generated from a heterozygous KI mouse (Figure 1). Real time PCR analysis further confirmed similar *Inf2* transcript levels in control and mutant mice (Figure 1f). We performed immunofluorescence and immunoblotting analysis of *Inf2* to examine the protein expression and localization in kidney. We observed that *Inf2* staining in the glomerulus is significantly reduced in the heterozygous and homozygous *Inf2* R218Q kidneys (Figure 1h). Consistent with this observation, immunoblotting analysis of glomerular lysates also showed a significant decrease in *Inf2* protein levels in heterozygous and homozygous mouse (Figure 1g), suggesting a loss of mutant protein post-synthesis (Figure 1f).

We attempted to express and purify the R218Q mutant in bacteria as a DID-containing N-terminal construct (amino acids 1-424 of murine INF2). While the wild-type construct expresses and folds efficiently (resulting in 3.6 mg of purified protein per liter of bacterial culture), the R218Q mutant yield was poor, with minimal protein present after full purification. These results suggest that, while the wildtype INF2 protein folds readily, the R218Q form folds poorly and is unstable (Figure 1i).

### Phenotype of INF2 R218Q knock-in mouse

As organs of the mutant mice appeared grossly normal, we limited our in-depth analysis to kidney structure and function. Our results showed that neither heterozygous (*Inf2*<sup>R218Q/+</sup>) nor homozygous (*Inf2*<sup>R218Q/R218Q</sup>) "knockin" (or "KI" mice, as we will refer to these lines subsequently) showed significant proteinuria or decreased kidney function as measured by serum creatinine (Supplementary Fig 1a; n=5 in each group,  $p > 0.05$  WT/KI vs. WT/WT;  $p > 0.05$  KI/KI vs. WT/WT) up to 15 months of age. The absence of significant proteinuria was confirmed by SDS-PAGE of urine samples (Supplementary Figure 1b).

We did not observe any glomerular damage by histology in heterozygous R218Q mice up to 12 months of age (Figure 2). Ultrastructurally, we observed some slight irregularities in foot processes from the R218Q/R218Q mice, though most of the podocytes appeared normal with intact foot processes and normal slit diaphragm structure. Immunofluorescence staining and immunogold labeling show normal slit diaphragm localization of nephrin in R218Q podocytes as well as in those from littermate control mice (Figure 3).

### INF2 R218Q mutation impairs slit diaphragm and podocyte recovery from protamine induced injury

We induced reversible podocyte injury in the mouse models (6 months of age) by means of perfusion with protamine sulfate (PS), followed by perfusion with heparin sulfate (HS) to neutralize the protamine. PS perfusion induced aberrant actin structures, which exhibited a

more aggregated pattern (Figure 2), foot process flattening, and characteristic narrowing of slit diaphragms regardless of *Inf2* genotype. HS perfusion restored the morphology of foot processes and slit diaphragms in control mice, whereas in both heterozygous and homozygous KI mice, the altered podocyte morphology and slit diaphragm structures did not recover.

To elucidate the impact of the R218Q mutation on the integrity of slit diaphragm protein complex in response to the protamine stress model, we compared the expression pattern of the slit diaphragm proteins nephrin and podocin by immunofluorescence staining and immunogold labeling. As shown in Figure 3, we observed similar linear distribution patterns of these proteins in mice of the different *Inf2* genotypes following either HBSS or PS perfusion. However, after perfusion with PS followed by HS, we observed mislocalization and punctate staining for nephrin and podocin in heterozygous and homozygous KI mice, compared to the more linear distribution in wild type mice (Figure 3).

As actin-based structures are essential for slit diaphragm formation and maintenance, and as *INF2* regulates actin polymerization<sup>4</sup>, we looked for changes in actin-based organization by staining for podocin, cortactin and F-actin in podocyte outgrowth cultures. Although significant differences were not seen in the central region of outgrown-colonies between genotypes, we observed clear changes at the edges. In particular, cell protrusion, lamellipodia formation, and cortactin distribution were altered (Figure 4). Irrespective of the *INF2* genotype, PS treatment of cells led to reduced lamellar protrusions, altered cortactin and podocin staining patterns (particularly at the plasma membrane), and increased F-actin structures throughout the cells. Subsequent HS treatments led to partial recovery of cell protrusions and peripheral cortactin staining in wild-type cells. In contrast, hetero- and homozygous KI cells did not show a significant response to HS treatment.

### **R218Q mutation alters nephrin phosphorylation**

Phosphorylation of nephrin tyrosine residues Y1176/Y1193 has been shown to help mediate a nephrin/Nck interaction and maintain the integrity of the slit diaphragm<sup>16, 17</sup>. We therefore performed immunofluorescence staining and western blotting using an antibody against tyrosine-phosphorylated nephrin. We observed an increase in phosphorylation in PS perfused mice, irrespective of the *INF2* genotype (Figure 5a and d, \* $p < 0.05$  WT/WT, WT/KI, KI/KI perfused with PS *vs.* WT/WT perfused with HBSS). In wild-type mice, HS perfusion returned nephrin phosphorylation to near baseline levels. In contrast, there were sustained elevations in phosphorylated nephrin observed in both heterozygous and homozygous *Inf2* R218Q knockin mice (Figure 5). In addition, total and phosphorylated nephrin staining showed a distinct punctate pattern (Figures 3, 5).

### **Impaired recovery from PS induced podocyte changes associates with persistent mDia activity**

We compared the activity of Rho/Dia signaling in kidneys of mice with different *Inf2* genotypes in response to different treatments. Rho activity was measured by Rhotekin GBD pulldown assay and expressed as the ratio of the GTP bound Rho to total Rho. mDia activity was expressed as the ratio of the membrane-associated to total mDia. PS perfusion induced

an increase in both active Rho and mDia in mouse kidneys regardless of the genotype (Figure 5). The increased Rho activity induced by PS was reversed by HS perfusion in all genotypes (Figure 5). However, HS perfusion failed to reverse mDia activation in knockin mice, while it returned mDia activity to baseline levels in wild-type animals (Figure 4). Sustained mDia activation in KI animals correlates with the persistently abnormal podocyte morphology, slit diaphragm protein localization and nephrin phosphorylation seen in *Inf2* mutant animals despite HS perfusion. Taken together, our *in vivo* data support for a model wherein INF2 is required for podocyte recovery from transient injury, with the R218Q pathogenic mutation leading to persistent damage and ultimately irreversible disease upon podocyte injury/stress.

## Discussion

Genetic studies have identified cytoskeletal proteins which when mutated cause FSGS in humans<sup>1, 18</sup>. Mutations in INF2 appear to be the most common cause of autosomal dominant FSGS<sup>2</sup>. Typically, individuals with INF2-mediated disease manifest proteinuria in adulthood, with progressive deterioration in kidney function and development of ESRD within 10 years. Disease mutations are clustered in the amino-terminal diaphanous inhibitory domain (DID), which is thought to act as an intra- and intermolecular inhibitor of the diaphanous autoregulatory domain (DAD). *In vitro* experimental results suggest that the mutations cause a loss of inhibitory function with enhanced mDia activity, actin stress fiber formation and impaired slit-diaphragm protein trafficking<sup>5, 6</sup>. Here, we report the *in vivo* effects of introducing the FSGS-associated R218Q point mutation into the mouse *Inf2* gene.

Mice carrying the R218Q *Inf2* mutation maintain normal glomerular function. Homozygous animals demonstrate only minimal glomerular or podocyte pathology: we observed mild patchy irregularity of the foot processes of the homozygous R218Q mice with slight cytoskeletal condensation compared with morphology seen in control and R218Q heterozygous mice. The lack of overt disease in mice with a R218Q mutation compared to humans may reflect several factors. INF2-associated disease in humans is relatively late in onset and demonstrates incomplete penetrance<sup>2</sup>. This is consistent with the notion that INF2 mutations do not directly alter glomerular development or function, but rather interfere with maintenance or repair processes. It may simply take many years for overt disease to develop or for the animal to be exposed to the necessary initiating injury. Alternatively, the lack of overt disease in the mouse may reflect broader differences in INF2 function between humans and mice. Ultimately, our findings in mice may be easier to reconcile with INF2-mediated human disease than with our previous studies in zebrafish, where mutant INF2 failed to rescue the glomerular defects caused by INF2 knockdown<sup>19</sup>. The discrepancy between the zebrafish and mouse phenotypes is particularly surprising as we found that the R218Q mutation induces a dramatic decrease in INF2 protein levels in the mouse. These differences may be explained by additional effects caused by INF2 morpholinos in zebrafish or by fundamentally different roles for INF2 in fish and mammalian glomerular development.

We were surprised by the finding that the R218Q mutation dramatically decreases INF2 protein levels in glomeruli. The presence of similar glomerular mRNA levels in wild-type and mutant animals, coupled with the poor yields of bacterially expressed R218Q INF2

protein fragments, suggests that this is due to diminished protein stability. Confirmation of this point will require assessment of INF2 protein half-life in future *in vitro* experiments. Planned comparisons between INF2 R218Q homozygous mutant and INF2 knock-out animals will help address whether the phenotype described here represents a near null-allele or whether residual mutant INF2 protein plays an active role in mediating pathology.

Our *in vivo* and *in vitro* experiments together suggest that INF2 mutations, rather than inducing podocyte damage, prevent recovery from otherwise transient podocyte stress or injury. Variable exposure to such stressors may contribute to the variability in disease onset seen in families carrying the same INF2 mutations. Characterizing the response of R218Q INF2 mutant animals in additional transient podocyte injury models will help address this possibility as well as identify more physiological relevant signals capable of initiating INF2 mediated glomerular disease.

Our previous *in vitro* work has led us to hypothesize that INF2 acts as an inhibitor of mDia mediated actin cytoskeletal rearrangements downstream of RhoA. In this model, INF2 may act to maintain lamellipodial structures and permit trafficking of slit diaphragm proteins and lipid raft structures to the cell surface. *In vivo*, protamine sulfate perfusion has been utilized as a model of rapid and reversible foot process effacement. Loss of various actin cytoskeleton modulators, including Rac<sup>20</sup>, cofilin-1<sup>21</sup> and Crk1/2 and CrkL<sup>22</sup>, have been shown to prevent both foot process effacement *in vivo* and lamellipodia formation *in vitro* in response to protamine sulfate. In contrast to these previous findings, in our studies lack of recovery of lamellipodial protrusions after heparin sulfate recovery in mutant INF2 podocyte outgrowths correlated with impaired recovery of foot process architecture *in vivo*. Furthermore, *in vivo* analysis demonstrated enhanced RhoA activation in response to protamine sulfate, followed by return to baseline levels after heparin sulfate infusion. Of course, great caution is required in correlating effects on lamellipodia formation in cells with foot process effacement *in vivo*.

We have also found that protamine sulfate induced increased nephrin phosphorylation at tyrosines Y1176/Y1193 *in vivo* regardless of *Inf2* genotype. Rapid dephosphorylation of nephrin was observed following HS perfusion in the control mice. Both of these findings are in agreement with recently published results<sup>17</sup>. Meanwhile, in R218Q INF2 mice, nephrin phosphorylation failed to decrease following HS perfusion. This finding is consistent with prior *in vitro* findings that wild-type INF2 is involved in trafficking nephrin and associated lipid rafts to the plasma membrane<sup>6</sup> and that phosphorylation of nephrin triggers a raft-mediated endocytic pathway responsible for nephrin internalization<sup>23</sup>. Complicating such an interpretation is the finding that mice carrying a triple tyrosine to phenylalanine mutation in the nephrin cytoplasmic domain (corresponding to human Y1176F, Y1193F, and Y1217F, and preventing phosphorylation at these sites) have a similar response as R218Q INF2 animals in the protamine sulfate model – effacement in response to PS with impaired recovery after HS perfusion<sup>17</sup>. Reconciling these disparate results will require more detailed mechanistic studies of nephrin trafficking and phosphorylation. Our findings do suggest the R218Q mutant form of INF2 interferes with the dynamics of nephrin phosphorylation and turnover, either directly or indirectly, and result in impaired slit-diaphragm recovery after protamine sulfate.



In summary, we have demonstrated that an R218Q mutation in mouse INF2 impairs the recovery of podocyte from PS-induced podocyte injury (Figure 6). We observed a decrease in inactivation of mDia as well as prolonged nephrin tyrosine phosphorylation and sequestration of phosphorylated nephrin within punctate structures in the podocyte. These results are consistent with earlier *in vitro* findings that the R218Q mutation prevents INF2 from opposing Rho/mDia mediated actin dynamics and preserving the actin-dependent podocyte phenotype. We suspect that these observations are not unique to this particular FSGS-associated point mutation but are likely common to all human FSGS-associated mutations in the INF2 DID. Whether these findings are simply mediated by the decrease in total INF2 protein levels seen with the mutant protein or represent additional “gain-of-function” effects remains unresolved. The lack of phenotype in the unstressed animal suggests a model whereby altered INF2 function caused by these mutations becomes clinically significant only after a pathologic stressor, such as protamine sulfate, leads to increased Rho signaling. The impaired recovery from transient insults may help explain the susceptibility of individuals with INF2 mutations to podocyte injury and FSGS, and may also explain the variable age of disease onset and penetrance. These findings also suggest that methods to down-modulate Rho and mDia mediated signaling in the podocyte could provide therapeutic approaches for some forms of glomerular injury.

## Materials and methods

### Generation of knock in mouse model

INF2 knockin mice were by the Velocigene method<sup>24</sup>. A BAC-based targeting construct was generated with the arginine 218 (CGG) to glutamine (CAG) replaced codon and a neomycin (Neo) resistance cassette flanked by loxP sites in intron 4/5. After selection, Neo cassette was removed by Cre-mediated recombination, leaving a single LoxP site. Correctly targeted ES cells were injected into 8-cell Swiss Webster embryos (Charles River Laboratories) as previously described<sup>25</sup>. Embryos were cultured overnight and transferred into pseudopregnant female mice 2.5 days post coitus. F0 generation male mice were bred with C57BL/6 mice to generate heterozygous and homozygous R218Q mice<sup>24, 25</sup>.

Mice were genotyped for the R218Q by PCR (Figure 1). Kidney RNA was extracted using an RNeasy Mini Kit (Qiagen), and reverse transcribed by an oligo dT primer followed by RT-PCR using primers flanking the mutated site. Transcription of the mutated allele was confirmed by sequencing of the RTPCR product obtained from heterozygous mice (Figure 1). For real time PCR analysis, RNA was extracted from glomerulus preparations, and reverse transcribed. The following primers: Inf2 F: CTGAAGGAGAACAAGGACCG, R-TGACGCACACCTCTTCTTG; Nephrin F: GGAAGGAGACAGTGCTAAAGG, R-GGGAAACTAGGATGGAGAGGATTAC were used in a SYBR green PCR assay.

### Measurement of urine albumin and serum creatinine

We collected urine and blood samples from 5 mice of each Inf2 genotype (WT/WT, WT/KI, KI/KI littermates) at various ages. Proteinuria was measured as the ratio of albumin to creatinine in urine samples (Siemens DCA2000+ microalbumin/creatinine kit). Serum creatinine was determined using Mouse Creatinine Enzymatic Assay Kit (Crystal Chem Inc.

IL). Two  $\mu\text{l}$  of urine from each sample was analyzed by SDS-PAGE followed by Coomassie Blue staining to detect urinary proteins.

### **Protamine sulfate perfusion**

Mouse kidney perfusions with protamine sulfate were carried out on 6-month old mice as described previously<sup>26</sup>. After perfusion, one kidney was dissected for histology, ultrastructure and molecular biology study. The other was used for glomerular isolation. Perfusions were repeated in three independent experiments. The local IACUC approved the animal experiments. Work was conducted in accord with the NIH Guidelines for the Care and Use of Experimental Animals.

### **Transmission electron microscopy**

Mouse kidney tissues were immersion fixed in 2.5% glutaraldehyde, 2% paraformaldehyde, in 0.1M Cacodylate buffer pH 7.4 (modified Karnovsky's fixative). They were post-stained in 1% osmium tetroxide, dehydrated, and embedded in Epon for thin sectioning and TEM study. For immunogold, eighty-nm sections were placed on carbon coated and glow discharged formvar coated nickel slot grids. Blocked grids were incubated in a rabbit anti-podocin antibody (P0372, Sigma Aldrich) or a rabbit anti-nephrin antibody (PRS2265, Sigma Aldrich) at room temperature, followed by a gold-conjugated antirabbit IgG (Abcam). After fixing with 1% glutaraldehyde in TBS, sections were contrast stained with uranyl acetate. Grids were imaged on a JEOL 1400 TEM.

### **Immunofluorescence staining**

Formalin-fixed, paraffin-embedded kidney sections were de-paraffinized and rehydrated, followed by antigen retrieval in heated Sodium Citrate Buffer (10mM Sodium Citrate, 0.05% Tween 20, pH 6.0). The sections were blocked in 10% FCS and sequentially incubated with indicated primary and secondary antibodies (Supplemental Table 1). Podocyte outgrowth cultures were fixed and stained with indicated antibodies. Counterstaining visualized F-actin and the nucleus. After mounting, the sections were imaged by confocal microscopy.

### **Isolation of glomeruli and podocyte outgrowth culture**

Kidneys were minced and pressed through a 100- $\mu\text{m}$  cell strainer and a 40- $\mu\text{m}$  cell strainer successively. The glomeruli recovered in the 40- $\mu\text{m}$  cell strainer were collagenase digested (1 mg/ml collagenase A in HBSS) at 37°C for 3 minutes, washed with HBSS and collected by centrifugation at  $200 \times g$  for 5 minutes. The isolated glomeruli were used for measurements of Inf2, Rho activation, membrane/total mDia, and nephrin phosphorylation. Experiments were repeated three independent times. For podocyte outgrowth cultures, glomeruli were isolated from HBSS perfused kidneys as described above and plated on fibronectin-coated surface. After 7 days of culture, the outgrown podocytes were subjected to PS (100  $\mu\text{g}/\text{mL}$  – 1 hr) and HS (500  $\mu\text{g}/\text{mL}$  – 2 hr) treatments prior to fixation and immunofluorescence microscopy.



### Cell protrusion measurements

Cells stained for cortactin, podocin, and F-actin were imaged for measuring cell protrusions as shown in Supplementary Figure 2. Measurements were made using Zeiss Confocal software (ZEN lite version 2). Cell protrusions were defined as regions from the edge of the cell to the verge of podocin-rich staining. These regions of interest were marked directly in the acquired images using “draw spline contour tool” and their perimeters were noted as outer perimeter (cell-edge) and inner perimeter (podocin staining). The difference between the perimeters was represented as percent protrusive values. At least five different colonies, with all cells along each colony edge measured, were included for analysis. As podocytes grown out from glomeruli are highly heterogeneous, we limited our analysis to colonies with podocin-positive staining and a cobblestone appearance of cells<sup>27</sup>.

### Rho activation Assay

Rho activity in isolated mouse glomerular extracts was measured using a Rhotekin RBD pulldown assay using the Rho Activation Assay Kit (EMD Millipore). The ratio of GTP-bound to total Rho was used as an index for Rho activity<sup>6</sup>.

### Quantification of membrane associated mDia

The membrane fraction of isolated mouse glomeruli was isolated as described<sup>6</sup>. The amount of mDia protein in the membrane fraction and total glomerular lysates was measured by Western blot. The ratio of membrane-associated to total mDia was used as an index for active mDia.

### Nephrin phosphorylation

Mouse glomeruli were lysed in RIPA buffer (phosphate-buffered 0.9% NaCl containing 0.1% SDS, 1% NP-40, and 0.5% sodium deoxycholate) supplemented with 1× Complete, EDTA-free proteinase and Phosphatase Inhibitor Cocktail (Roche Molecular Biochemicals). Equal amounts of protein were then separated by SDS-PAGE and analyzed for phosphorylated and total nephrin levels using indicated antibodies (Supplemental Table 1).

### Statistical analysis

Data analyses were performed using SPSS version 10.0. Urine ACR, serum creatinine, and the densitometric analysis of Rho, mDia and nephrin using NIH Image J are expressed as mean ± SE. Oneway Anova was used for comparisons among multiple groups, and q test was used to compare the difference between groups. In a two-tailed test,  $p < 0.05$  was considered significant.

### Supplementary Material

Refer to Web version on PubMed Central for supplementary material.

### Acknowledgments

We thank Suzanne L. White, Andrea Calhoun, Yi Zheng, Lay-Hong Ang from the Histology Core, EM Core and Confocal Core at BIDMC for their help in experiments. This work was supported by grant NIH DK008826.

## REFERENCES

1. Brown EJ, Schlondorff JS, Becker DJ, et al. Mutations in the formin gene INF2 cause focal segmental glomerulosclerosis. *Nat Genet.* 2010; 42:72–76. [PubMed: 20023659]
2. Barua M, Brown EJ, Charoonratana VT, et al. Mutations in the INF2 gene account for a significant proportion of familial but not sporadic focal and segmental glomerulosclerosis. *Kidney international.* 2013; 83:316–322. [PubMed: 23014460]
3. Boyer O, Benoit G, Gribouval O, et al. Mutations in INF2 are a major cause of autosomal dominant focal segmental glomerulosclerosis. *J Am Soc Nephrol.* 2011; 22:239–245. [PubMed: 21258034]
4. Chhabra ES, Higgs HN. INF2 Is a WASP homology 2 motif-containing formin that severs actin filaments and accelerates both polymerization and depolymerization. *J Biol Chem.* 2006; 281:26754–26767. [PubMed: 16818491]
5. Sun H, Schlondorff JS, Brown EJ, et al. Rho activation of mDia formins is modulated by an interaction with inverted formin 2 (INF2). *Proceedings of the National Academy of Sciences of the United States of America.* 2011; 108:2933–2938. [PubMed: 21278336]
6. Sun H, Schlondorff J, Higgs HN, et al. Inverted formin 2 regulates actin dynamics by antagonizing Rho/diaphanous-related formin signaling. *J Am Soc Nephrol.* 2013; 24:917–929. [PubMed: 23620398]
7. Kubiak A, Niemir ZI. The role of podocytes in normal glomerular function and in the pathogenesis of glomerulonephritis. Part I. Phenotypic and functional characteristics of podocytes during their differentiation and maturity]. *Postepy Hig Med Dosw (Online).* 2006; 60:248–258. [PubMed: 16702924]
8. Asanuma K, Mundel P. The role of podocytes in glomerular pathobiology. *Clin Exp Nephrol.* 2003; 7:255–259. [PubMed: 14712353]
9. Zhu L, Jiang R, Aoudjit L, et al. Activation of RhoA in podocytes induces focal segmental glomerulosclerosis. *J Am Soc Nephrol.* 2011; 22:1621–1630. [PubMed: 21804090]
10. Scott RP, Hawley SP, Ruston J, et al. Podocyte-specific loss of Cdc42 leads to congenital nephropathy. *J Am Soc Nephrol.* 2012; 23:1149–1154. [PubMed: 22518006]
11. Akilesh S, Suleiman H, Yu H, et al. Arhgap24 inactivates Rac1 in mouse podocytes, and a mutant form is associated with familial focal segmental glomerulosclerosis. *The Journal of clinical investigation.* 2011; 121:4127–4137. [PubMed: 21911940]
12. Mouawad F, Tsui H, Takano T. Role of Rho-GTPases and their regulatory proteins in glomerular podocyte function. *Canadian journal of physiology and pharmacology.* 2013; 91:773–782. [PubMed: 24144047]
13. Oh J, Reiser J, Mundel P. Dynamic (re)organization of the podocyte actin cytoskeleton in the nephrotic syndrome. *Pediatric nephrology.* 2004; 19:130–137. [PubMed: 14673634]
14. Shono A, Tsukaguchi H, Kitamura A, et al. Predisposition to relapsing nephrotic syndrome by a nephrin mutation that interferes with assembly of functioning microdomains. *Human molecular genetics.* 2009; 18:2943–2956. [PubMed: 19443487]
15. Gupta IR, Baldwin C, Auguste D, et al. ARHGDI1: a novel gene implicated in nephrotic syndrome. *Journal of medical genetics.* 2013; 50:330–338. [PubMed: 23434736]
16. Jones N, New LA, Fortino MA, et al. Nck proteins maintain the adult glomerular filtration barrier. *J Am Soc Nephrol.* 2009; 20:1533–1543. [PubMed: 19443634]
17. New LA, Martin CE, Scott RP, et al. Nephrin Tyrosine Phosphorylation Is Required to Stabilize and Restore Podocyte Foot Process Architecture. *J Am Soc Nephrol.* 2016
18. Kaplan JM, Kim SH, North KN, et al. Mutations in ACTN4, encoding alpha-actinin-4, cause familial focal segmental glomerulosclerosis. *Nat Genet.* 2000; 24:251–256. [PubMed: 10700177]
19. Sun H, Al-Romaih KI, MacRae CA, et al. Human Kidney Disease-causing INF2 Mutations Perturb Rho/Dia Signaling in the Glomerulus. *EBioMedicine.* 2014; 1:107–115. [PubMed: 26086034]
20. Blattner SM, Hodgkin JB, Nishio M, et al. Divergent functions of the Rho GTPases Rac1 and Cdc42 in podocyte injury. *Kidney international.* 2013; 84:920–930. [PubMed: 23677246]
21. Garg P, Verma R, Cook L, et al. Actin-depolymerizing factor cofilin-1 is necessary in maintaining mature podocyte architecture. *J Biol Chem.* 2010; 285:22676–22688. [PubMed: 20472933]

22. George B, Fan Q, Dlugos CP, et al. Crk1/2 and CrkL form a hetero-oligomer and functionally complement each other during podocyte morphogenesis. *Kidney international*. 2014; 85:1382–1394. [PubMed: 24499776]
23. Qin XS, Tsukaguchi H, Shono A, et al. Phosphorylation of nephrin triggers its internalization by raft-mediated endocytosis. *J Am Soc Nephrol*. 2009; 20:2534–2545. [PubMed: 19850954]
24. Valenzuela DM, Murphy AJ, Frendewey D, et al. High-throughput engineering of the mouse genome coupled with high-resolution expression analysis. *Nature biotechnology*. 2003; 21:652–659.
25. Poueymirou WT, Auerbach W, Frendewey D, et al. F0 generation mice fully derived from gene-targeted embryonic stem cells allowing immediate phenotypic analyses. *Nature biotechnology*. 2007; 25:91–99.
26. George B, Verma R, Soofi AA, et al. Crk1/2-dependent signaling is necessary for podocyte foot process spreading in mouse models of glomerular disease. *The Journal of clinical investigation*. 2012; 122:674–692. [PubMed: 22251701]
27. Krttil J, Platenik J, Kazderova M, et al. Culture methods of glomerular podocytes. *Kidney & blood pressure research*. 2007; 30:162–174. [PubMed: 17502717]

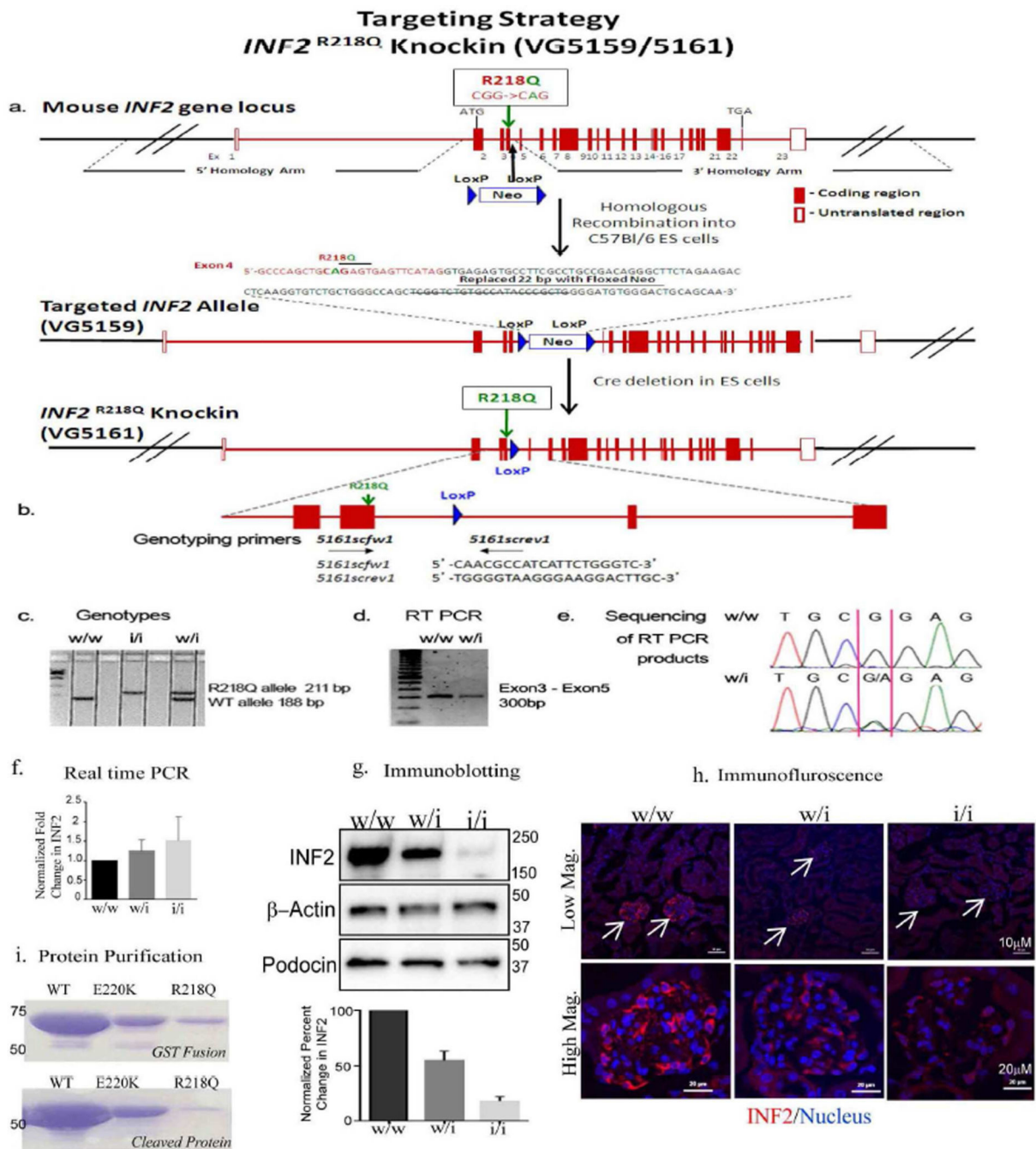


**Figure 1. *Inf2* R218Q knockin mouse targeting and genotyping strategy**

a. The R218Q mutation (in exon 4) was introduced into the mouse *Inf2* gene locus by homologous recombination to generate an *Inf2* R218Q knockin allele in C57Bl/6 embryonic stem cells. b. Primers used for genotyping. c. A representative gel electrophoresis figure shows the pattern of genotypes in R218Q knockin mice. d. The transcription of mouse *Inf2* was examined by RT-PCR, using a pair of primers flanking exon 3 and exon 5. e. Direct sequencing of the RT PCR products confirmed the successful knock-in of the R218Q mutation in *Inf2*. f. Real time PCR analysis of *Inf2* from RNA extracted from WT, WT/KI,

and KI/KI glomerular preparations and normalized to nephrin transcript levels. Result are from 3 independent glomerular lysate preparations. Inf2 transcript levels were not statistically different between control and mutant mice. g. Immunoblot of INF2 from WT, WT/KI, and KI/KI glomeruli. A significant reduction of INF2 is seen in WT/KI and KI/KI glomeruli. Podocinnormalized quantification from three independent glomerulus preparations and a representative blot image are shown. h. Immunofluorescence staining of INF2 from WT, WT/KI, and KI/KI kidneys. i. Coomassie-stained gels of bacterially-expressed and purified constructs of INF2 amino acids 1-424 (mass 46.5 kDa). Wild-type, E220K and R218Q mutants analyzed. Top: constructs prior to cleavage of glutathione-S-transferase (GST) tag. Bottom: constructs after cleavage of GST tag. Equivalent volumes of purified fractions were loaded onto the gel.



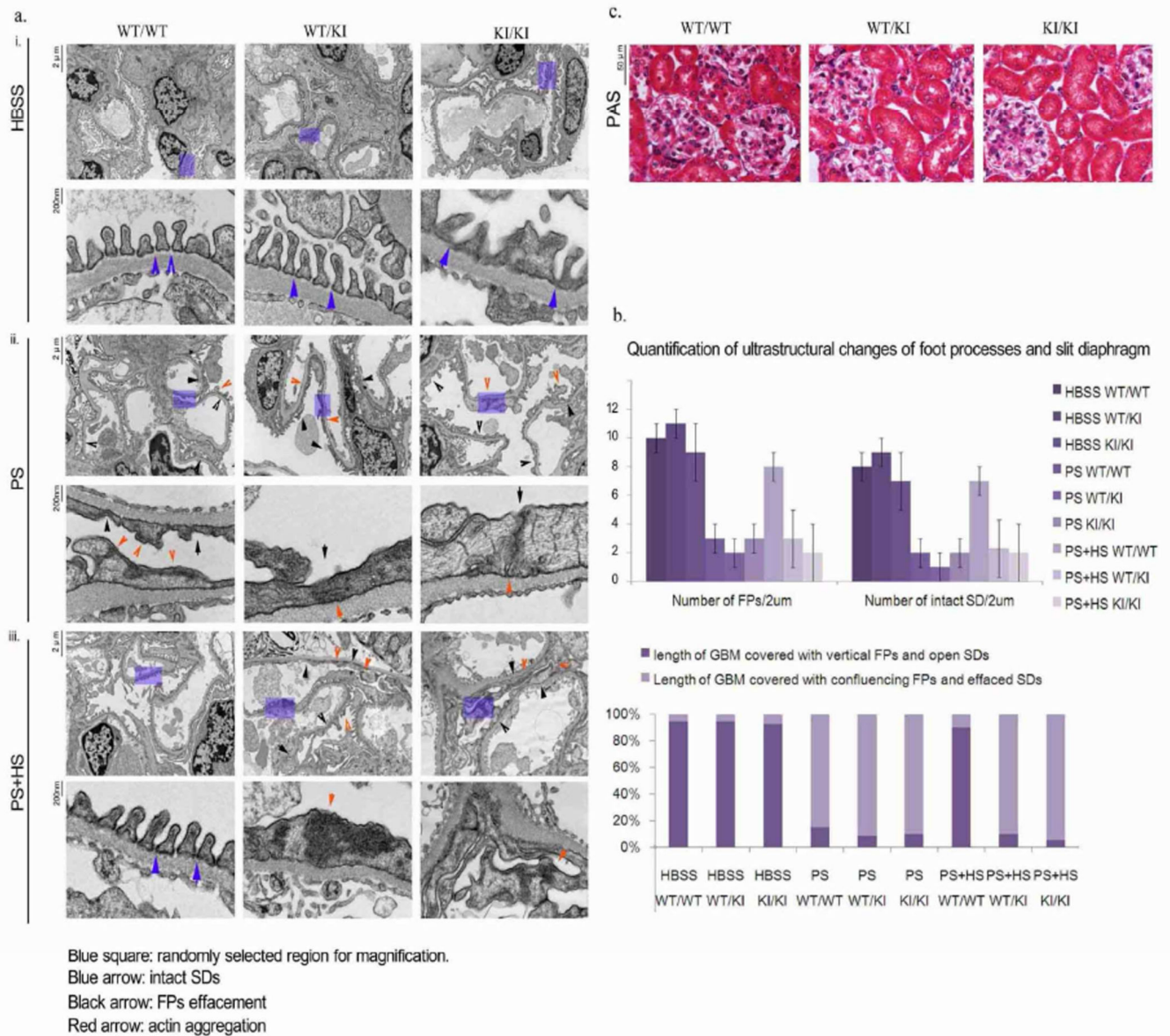


**Figure 2. Ultrastructural changes of podocytes in R218Q transgenic mouse following protamine sulfate/heparin sulfate perfusion**

Mice of different genotypes (WT/WT, WT/KI, KI/KI) were anesthetized at 6 months of age, followed by one of the following perfusions: i. HBSS (control group), ii. Protamine sulfate (injury group), iii. Protamine sulfate followed by heparin sulfate (rescue group). a. Transmission electron microscopy (TEM) images showing podocyte foot processes and slit diaphragms. Blue arrows, intact slit-diaphragm; black arrow, areas of effacement and abnormal cell-cell junctions; red arrow, cytoplasmic actin aggregates b. Quantification of foot process and slit diaphragm changes as observed by TEM. c. PAS stain of kidney sections from 6 month old animals of different genotypes (WT/WT, WT/KI and KI/KI) shows no significant gross glomerular abnormality under light microscopy.



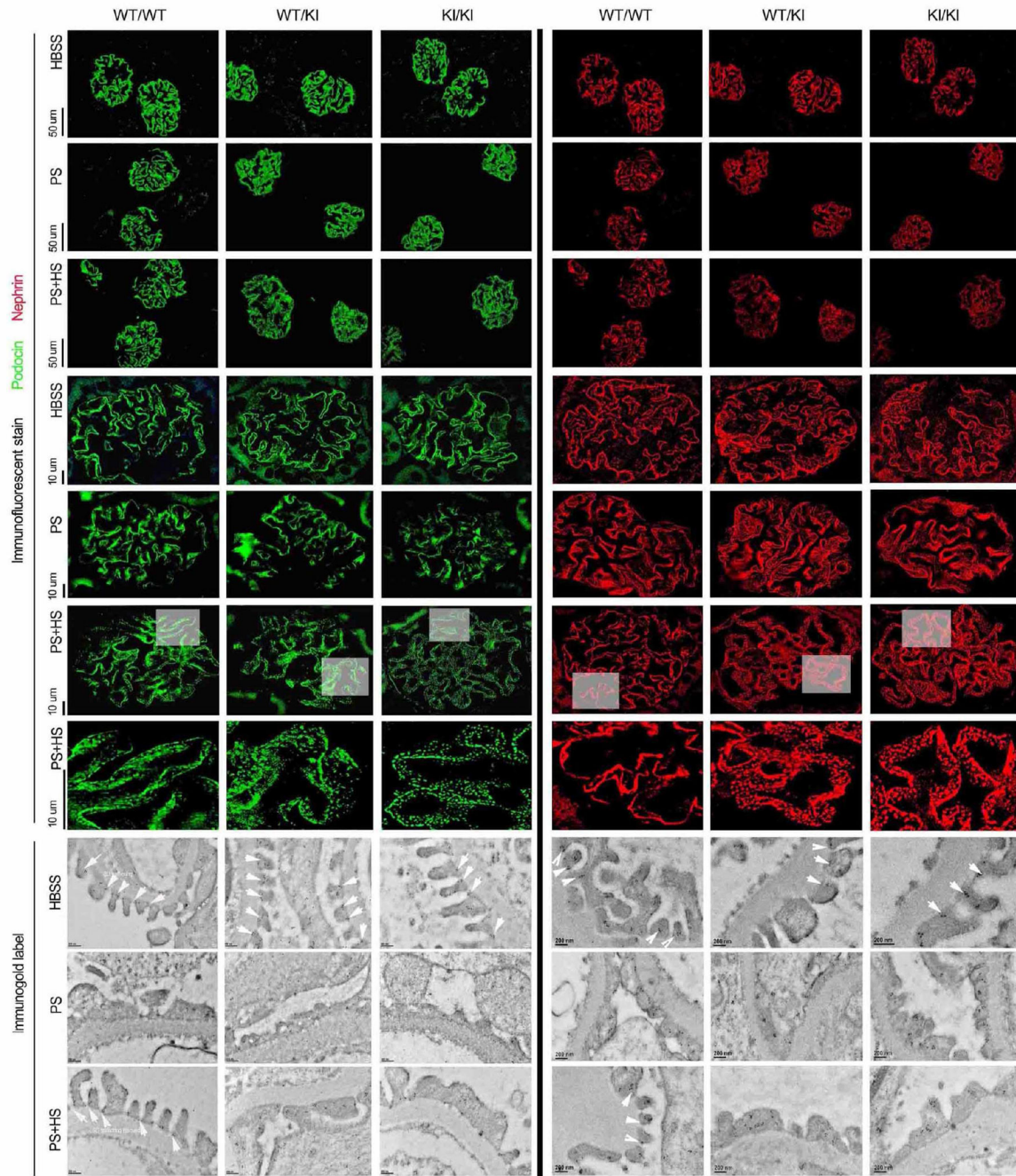
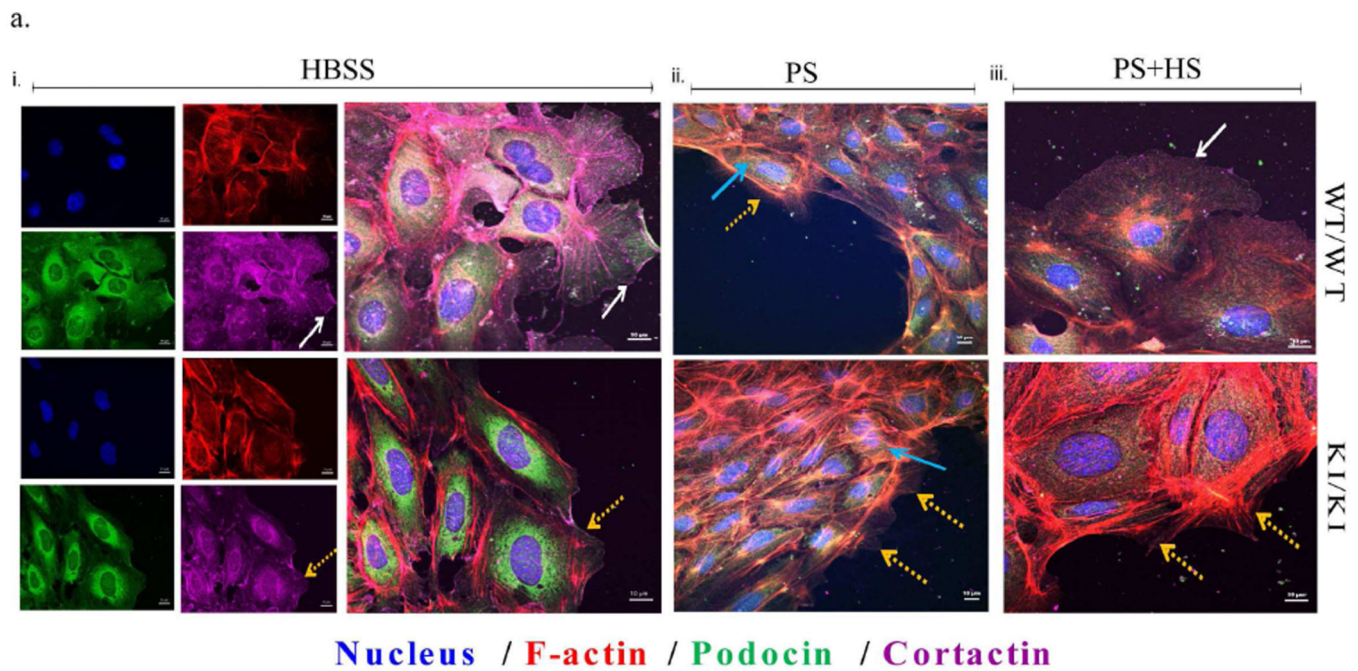


### Figure 3. Nephlin and podocin distribution

Distribution of slit diaphragm proteins podocin (left) and nephrin (right) in wild-type (WT/WT) and heterozygous (WT/KI) or homozygous (KI/KI) *Inf2* R218Q point mutant mice. Representative immunofluorescence and immunogold images are shown after control (HBSS), protamine sulfate (PS), or protamine sulfate followed by heparin sulfate (PS+HS) perfusion. Arrow highlights in immunogold EM images indicate podocin and nephrin gold particles in slit diaphragm region.



b. Quantification of Cell Protrusion in Podocyte-Outgrown Cultures

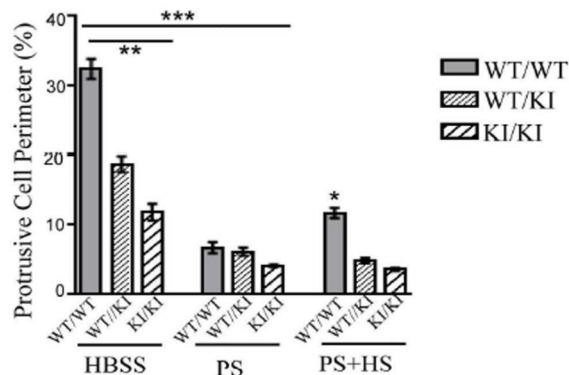


**Figure 4. Podocyte outgrowth cultures**

Podocyte outgrowth cultures from wild-type, heterozygous and homozygous *Inf2* R218Q mice were subjected to i. HBSS (control group), ii. Protamine sulfate (injury group), or iii. Protamine sulfate followed by heparin sulfate (rescue group) treatments, and stained for podocin (green), F-actin (red), cortactin (magenta) and nucleus (blue). a. Changes in cell protrusion/ lamellipodia and cortactin were noted and highlighted between groups. White arrows: continuous cortactin with large cell protrusion. Yellow arrows: discontinuous or absent cortactin staining and reduced cell protrusion/lamellipodia. Blue arrow: f-actin structures across the entire cell body. b. Quantification of cell protrusion/ lamellipodia between groups after different treatments. Calculation procedure is provided in supplementary figure 2. Controls cells exhibited significantly larger cell protrusion/ lamellipodia (\*\* $p < 0.05$  WT/WT vs WT/KI and KI/KI in HBSS). Protamine sulfate

significantly reduced the cell protrusions/ lamellipodia and cortactin (\*\* $p < 0.01$ , Respective HBSS vs PS treatment groups). Wild-type, but not WT/KI or KI/KI, cells showed partial recovery of protrusions after heparin sulfate treatment ( $p < 0.05$  WT in PS+HS vs WT in PS treatments).

Author Manuscript

Author Manuscript

Author Manuscript

Author Manuscript



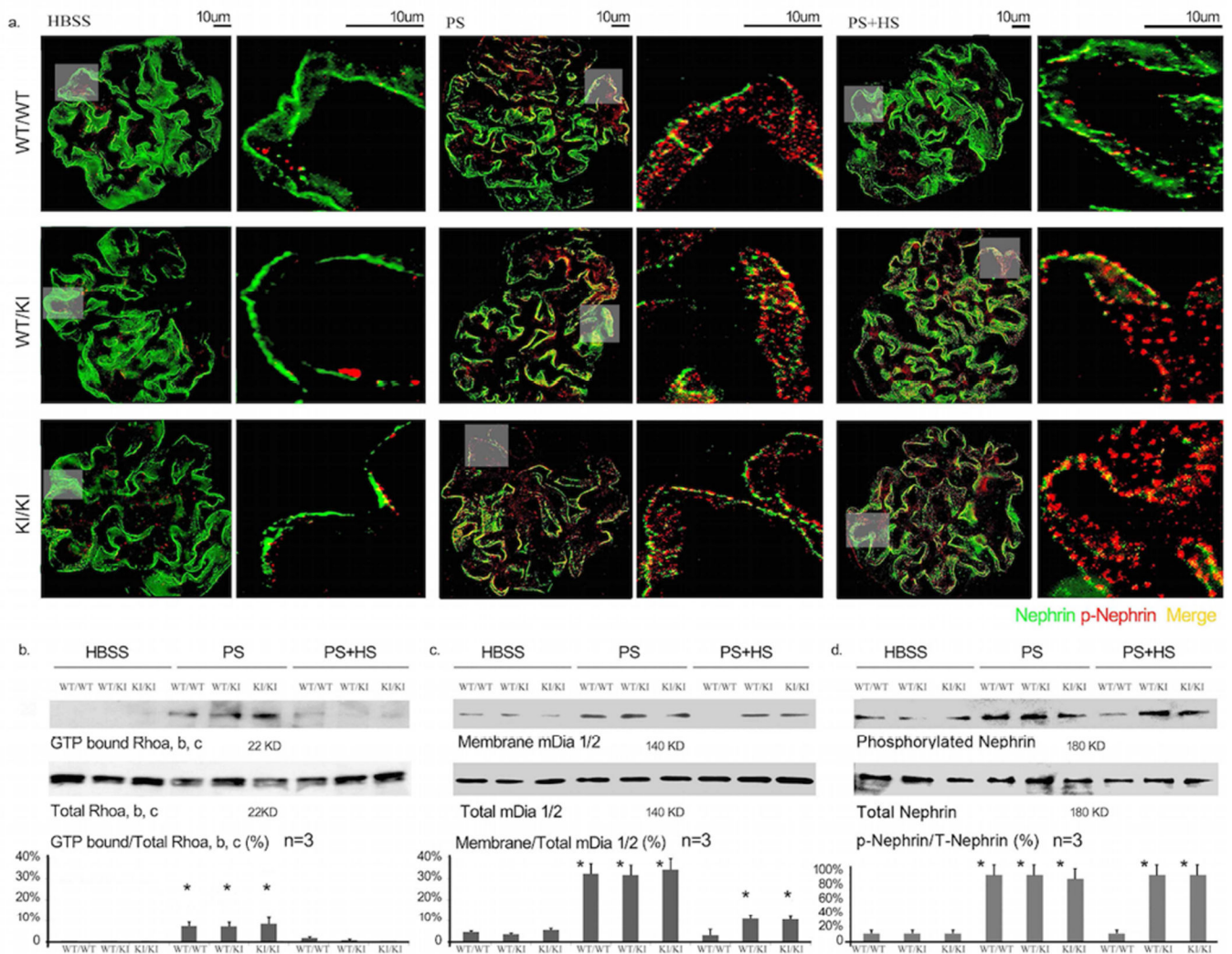


### Figure 5. Signaling activity

a. Immunofluorescence imaging of total nephrin and phosphorylated nephrin (phospho Y1176/Y1193) in glomeruli. Representative images are shown from wild-type (WT/WT), heterozygous (WT/KI) and homozygous (KI/KI) *Inf2* R218Q kidneys after perfusion with HBSS, protamine sulfate (PS) or protamine sulfate followed by heparin sulfate (PS+HS).

b,c,d: After different treatment, the mice were sacrificed, the kidneys were collected, and the glomeruli were isolated for quantitative analysis of Rho activity, mDia activity and nephrin phosphorylation. b. Rho activity was measured as the ratio of GTP bound / Total Rho. GTP bound Rho was measured using a Rhotekin GBD pulldown assay (\* $p < 0.05$ , WT/WT, WT/KI, KI/KI perfused with PS vs. WT/WT perfused with HBSS;  $p < 0.05$ , WT/WT, WT/KI, KI/KI perfused with PS+HS vs. corresponding genotype perfused with PS). c. Membrane-associated and the total amount of mDia were measured by Western blot. The mDia activity is expressed as the percentage of membrane mDia compared to total mDia. (\* $p < 0.05$ , WT/WT, WT/KI, KI/KI perfused with PS vs. WT/WT perfused with HBSS; \* $p < 0.05$  WT/KI, KI/KI perfused with PS+HS vs. corresponding genotype perfused with HBSS;  $p > 0.05$ , WT/WT perfused with PS+HS vs. WT/WT perfused with HBSS). d. Phosphorylated

and total nephrin were measured by Western blot. Nephrin phosphorylation is reported as a percentage compared to total nephrin (\* $p < 0.05$  WT/KI, KI/KI perfused with PS+HS vs. corresponding genotype perfused with HBSS;  $p > 0.05$  WT/WT perfused with PS+HS vs. WT/WT perfused with HBSS).

Author Manuscript

Author Manuscript

Author Manuscript

Author Manuscript

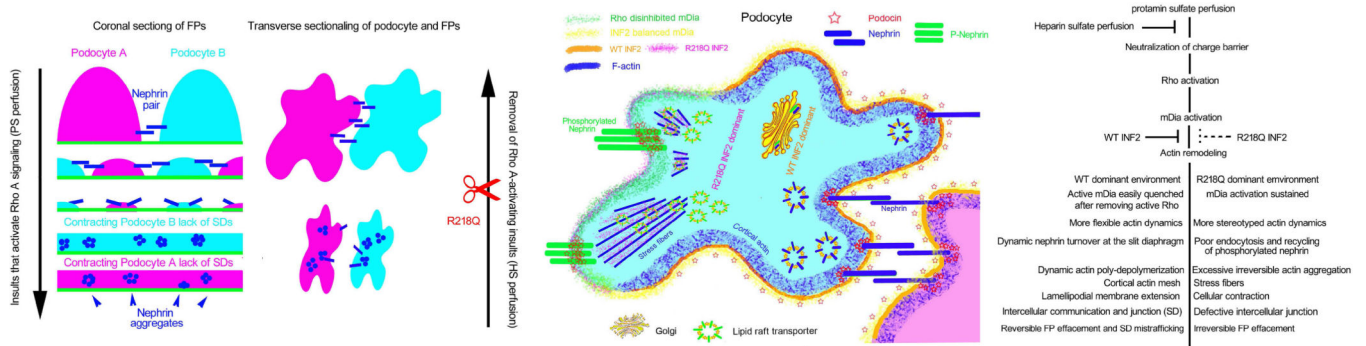


**Figure 6. Schematic of INF2 Function in Podocytes**

In one possible model, insults activating RhoA (such as Protamine sulfate injury) cause podocytes to lose slit diaphragm integrity, perhaps in part by aberrant mDia activation and nephrin phosphorylation, which in turn lead to excessive abnormal actin structures and foot process effacement. Subsequent removal of Rho A activation (such as heparin sulfate rescue) restores the slit diaphragm, perhaps by restoring the balance in mDia and nephrin phosphorylation. However, with the R218Q mutation, inhibition of the Rho A effector mDia signaling is decreased.